Supplemental Figure 1

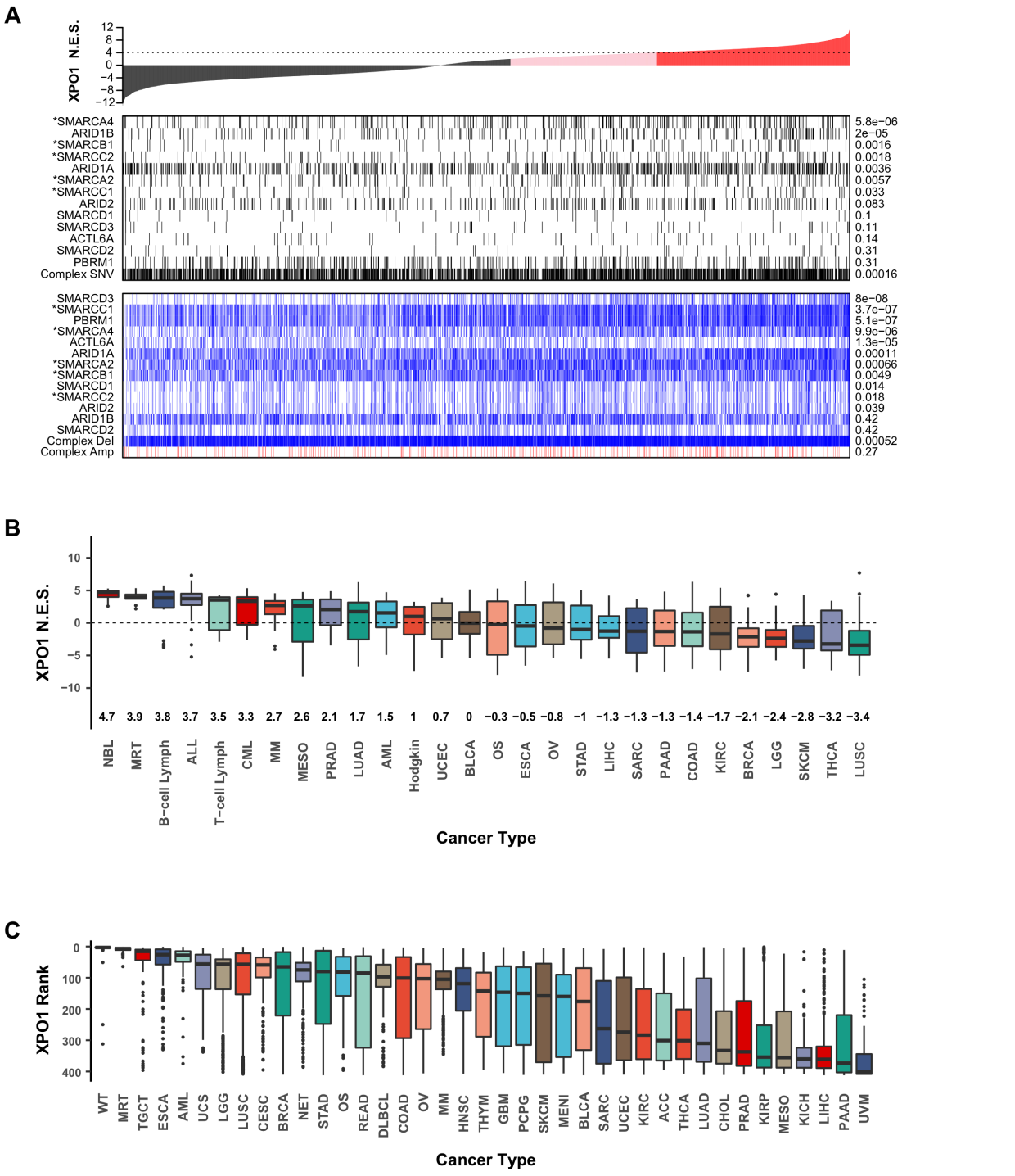

Figure S1. XPO1 activity across different tumor types and cell line models [Related to Figure 1]. A) Co-segregation analysis of SNV and CNV events in SWI/SNF complex genes with XPO1 activity. XPO1 activation occurs in association with mutations in SWI/SNF complex. Oncoprint (top) describing single nucleotide variants (SNVs) in SWI/SNF complex genes and in core subunits (SMARCA4 and SMARCB1, ARID1B) co-segregate with XPO1 activation. Estimated p-values from enrichment analysis are to the right. Oncoprint (bottom): CNV are more common than SNVs in SWI/SNF complex genes. Heterozygous (light blue) and homozygous (dark blue) deletions in several SWI/SNF complex genes cosegregate with increased XPO1 activity, as do amplifications (red). B) Boxplots representing the distribution of metaVIPER inferred XPO1 activity in a cohort of nine rhabdoid (MRT and ATRT) cell lines compared to 27 cohorts of cancer cell lines profiled in the publicly available CCLE. The median and interquartile range for NES values is represented by each box for the respective cell line cohort. NES values from enrichment analysis are comparable to Z-scores, with higher scores representing increased activity. C) XPO1 prediction rank for each TCGA/TARGET cohort.

Supplemental Figure 2

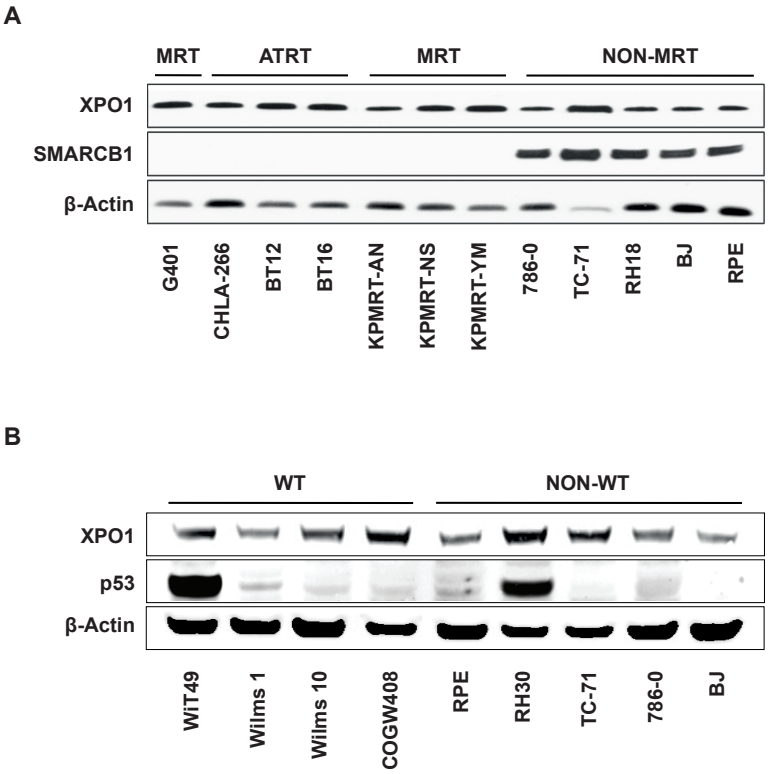

Figure S2. XPO1 protein expression across MRT, WT, and control cell lines [Related to Figure 2]. A) Protein expression of XPO1 and SMARCB1 across MRT, ATRT, and non-MRT cell lines. B) Protein expression of XPO1 and p53 across Wilms tumor and non-Wilms tumor cell lines. The non-MRT and non-WT cell lines comprise both malignant (786-0 – renal cell carcinoma, TC-71 – Ewing sarcoma, RH18 – Fusion positive rhabdomyosarcoma, RH30 – Fusion positive rhabdomyosarcoma) and non-malignant cell lines (BJ - fibroblast, RPE – TERT-immortalized retinal pigment epithelial cell).

Supplemental Figure 3

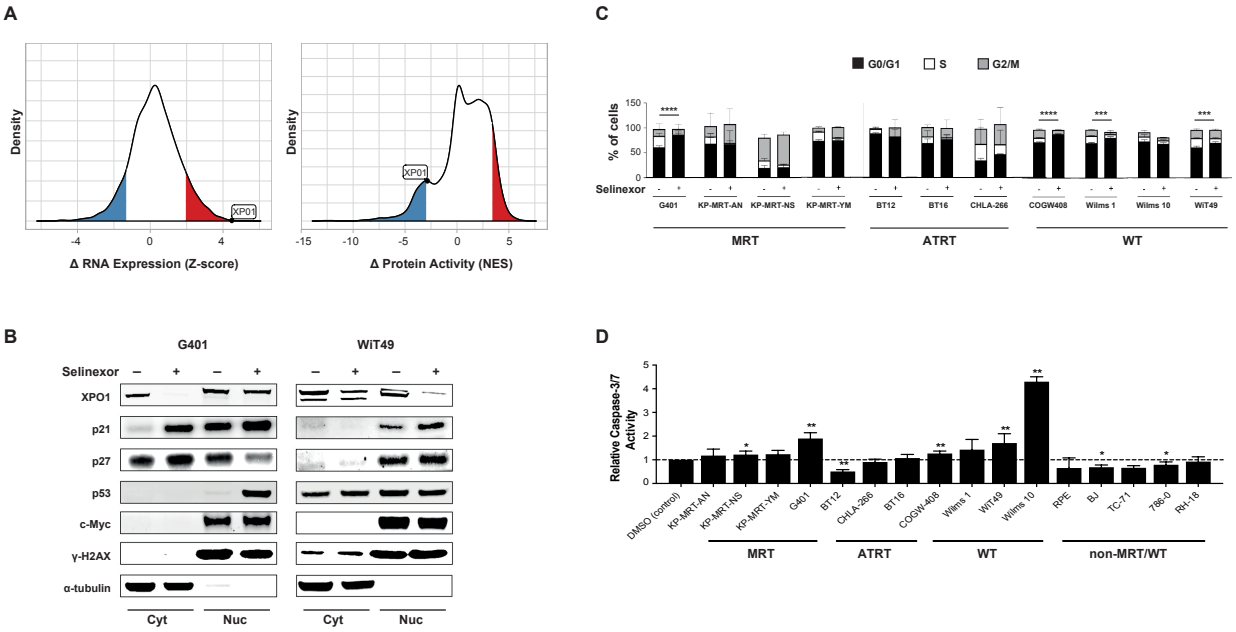

Figure S3. Effect of XPO1 pharmacological inhibition in MRT and WT cell lines [Related to Figure 2]. A) Change in mRNA (left) and the change in protein activity (right) of XPO1 following treatment with selinexor. Reduction in XPO1 inferred activity was noted along with a compensatory increase in XPO1 mRNA expression following treatment. B) Immunoblot showing expression levels and subcellular localization of XPO1 targets in G401 and WiT49 cell lines treated with selinexor. C) Cell cycle analysis of MRT and WT cell lines treated with DMSO (-) or selinexor (+). D) Relative caspase activity of MRT, WT and non- MRT/WT cell lines treated with selinexor. *=p<0.05, **=p<0.01, ***=p<0.001, ****=p<0.0001.

Supplemental Figure 4

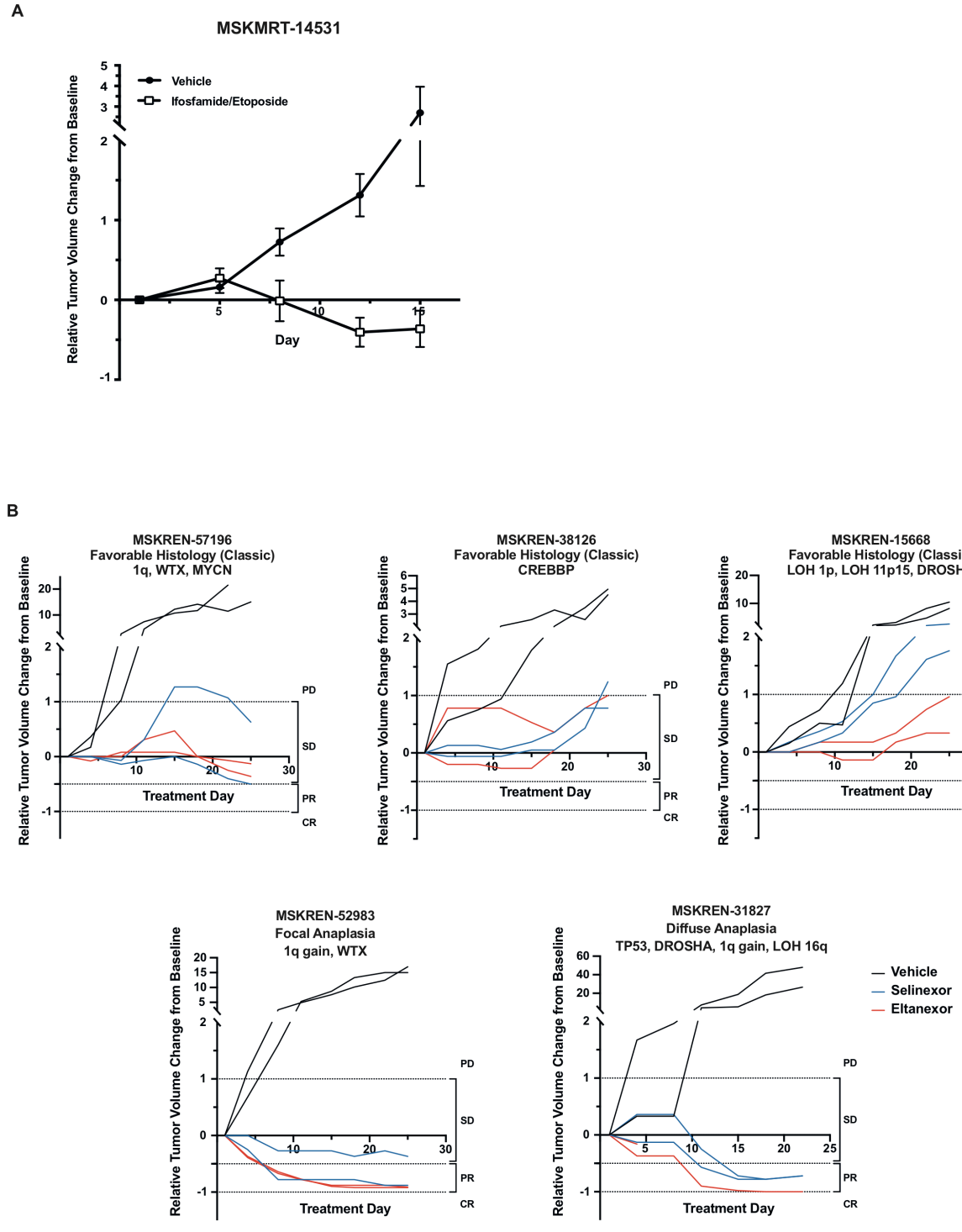

Figure S4. Tumor response of MRT and WT PDX models treated with selinexor and eltanexor [Related to Figures 3 and 4]. A) Tumor response of MRT (MSKMRT-14531) PDX treated with ifosfamide/etoposide for 15 days. Error bars: SEM. B) Relative tumor volume changes in Wilms tumor PDX models following treatment with selinexor (blue), eltanexor (red), or vehicle (black).

Supplemental Figure 5

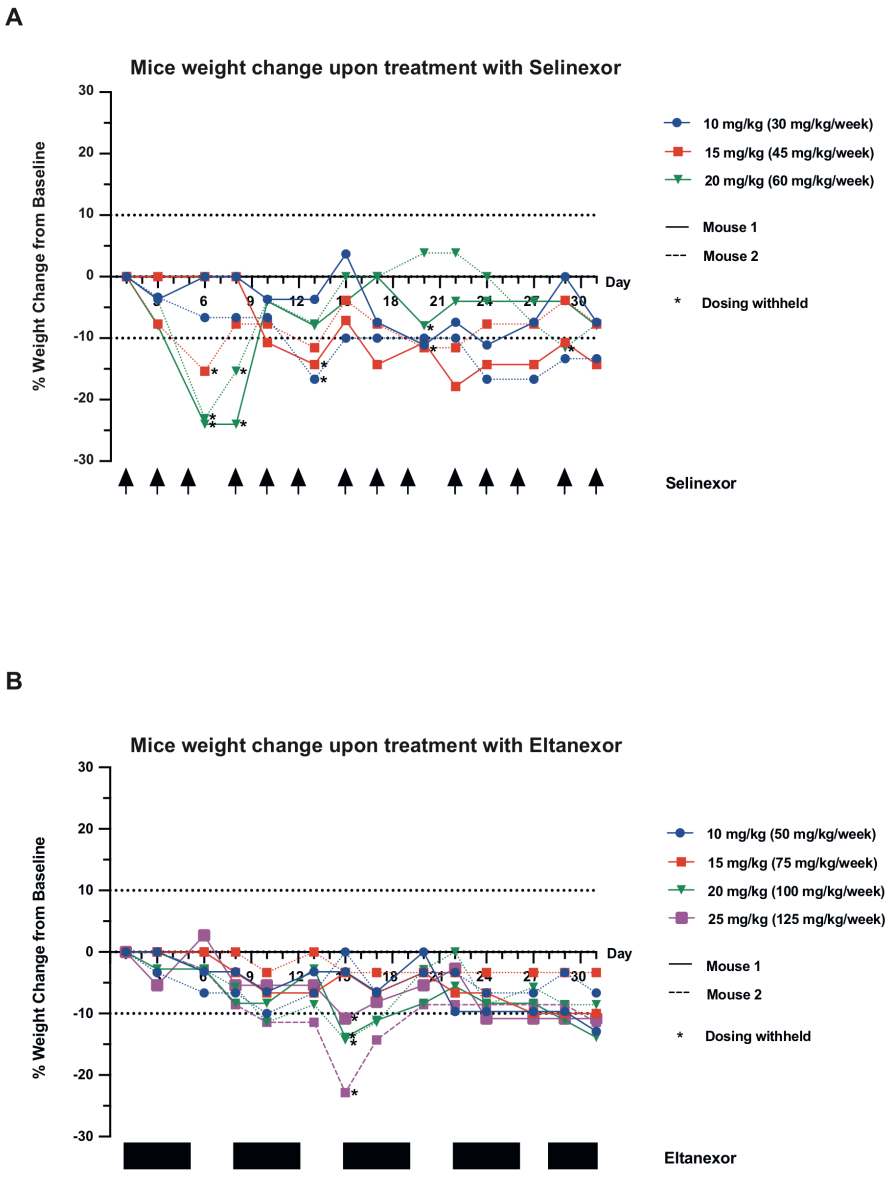

Figure S5. Tolerability of selinexor and eltanexor [Related to Figures 3 and 4]. Two mice were treated at each dose level for 31 days. A) Mice receiving selinexor were treated with thrice weekly dosing on a Monday, Wednesday, and Friday schedule. B) Mice receiving eltanexor were treated daily Monday through Friday. Asterix denotes days on which doses were held.

Supplemental Table 1. Cell line characteristics [Related to Figure 2 and STAR Methods].

Cell line	Disease/Tissue	TP53 status	IC_{50} Selinexor (nM)
COGW408	Wilms tumor (WT)	Wild type	114
Wilms 1	Wilms tumor (WT)	Wild type	91
Wilms 10	Wilms tumor (WT)	Wild type	26
WiT49	Wilms tumor (WT)	Mutant	207
KP-MRT-AN	Malignant Rhabdoid Tumor (MRT)	Wild type	143
KP-MRT-NS	Malignant Rhabdoid Tumor (MRT)	Mutant	296
KP-MRT-YM	Malignant Rhabdoid Tumor (MRT)	Wild type	89
G401	Malignant Rhabdoid Tumor (MRT)	Mutant	141
CHLA-266	Atypical Teratoid Rhabdoid Tumors (ATRT)	Mutant	368
BT12	Atypical Teratoid Rhabdoid Tumors (ATRT)	Mutant	1900
BT16	Atypical Teratoid Rhabdoid Tumors (ATRT)	Wild type	445
BJ	Fibroblast	-	48000
RPE	Retinal Pigment Epithelium	-	16500
RH-18	Rhabdomyosarcoma	Wild type	-
RH-30	Rhabdomyosarcoma	Mutant	122
TC-71	Ewing sarcoma	Mutant	515
786-O	Renal adenocarcinoma	Mutant	280

Supplemental Table 2. Summary of molecular alterations in MRT and WT models [Relate to STAR Methods].

Cell line / PDX	Gene	Protein Change	Mutation Type	**VAF** (%)
BT12	*ALOX12B*	-	CNA_DeepDel	-
	APC	A735V	Missense_Mutation	24.7
	APC	-	CNA_Amp	-
	ARID1B	P450dup	In_Frame_Ins	22.8
	ARID1B	I1602T	Missense_Mutation	54.1
	ARID2	I1322F	Missense_Mutation	49.1
	AURKB	-	CNA_DeepDel	-
	GPS2	-	CNA_DeepDel	-
	JAK2	I1051T	Missense_Mutation	45.4
	MAP2K1	R49C	Missense_Mutation	48.6
	PLCG2	A133V	Missense_Mutation	47.4
	SMARCB1	R60Efs*10	Frame_Shift_Del	92.2
	TP53	-	CNA_DeepDel	-
	ZRSR2	S447_R448dup	In_Frame_Ins	25
BT16	*BRCA1*	T374I	Missense_Mutation	48.3
	FOXA1	H168Q	Missense_Mutation	47.6
	HGF	X209_splice	Splice_Site	46.4
	IRS2	S144T	Missense_Mutation	48.6
	MSH3	A61_P63dup	In_Frame_Ins	36.9
	PIK3CB	H492R	Missense_Mutation	44.6
	SMARCB1	M27Rfs*28	Frame_Shift_Del	100.0
	SMO	L23dup	In_Frame_Ins	33.9
CHLA-226	*ARID1B*	P450dup	In_Frame_Ins	15.9
	ERBB4	A1236V	Missense_Mutation	50.1
	EWSR1-FLI1	-	Fusion	-
	FLI1-EWSR1	-	Fusion	-
	HIST1H2BD	M1?	Translation_Start_Site	48.1
	HIST1H3A	R129G	Missense_Mutation	47.2
	INPP4A	G226V	Missense_Mutation	42.2
	KDM5C	-	CNA_DeepDel	-
	KMT2C	P4726S	Missense_Mutation	52.3
	KMT2D	R5214C	Missense_Mutation	51.4
	MED12	P2135L	Missense_Mutation	7.5
	MYC	-	CNA_Amp	-
	PREX2	L368V	Missense_Mutation	24.6
	SMARCB1	R377H	Missense_Mutation	48.8
	SOCS1	E91K	Missense_Mutation	51.0
	TP53	R213*	Nonsense_Mutation	100.0
	TP53BP1	M521L	Missense_Mutation	50.7
G401	*AXL*	A572T	Missense_Mutation	43.8
	CYLD	Q729H	Missense_Mutation	52.9
	ESR1	S137R	Missense_Mutation	49.7
	SMARCB1	-	CNA_DeepDel	-
	TP53	C277F	Missense_Mutation	2.8

KP-MRT-NS	*EIF1AX*	G8R	Missense_Mutation	51.3
	EPHA5	D20N	Missense_Mutation	57.6
	ERCC4	R670Q	Missense_Mutation	55.1
	MSH2	L811F	Missense_Mutation	44.3
	MSH3	A61_P63dup	In_Frame_Ins	36.6
	PLK2	P52L	Missense_Mutation	52.5
	RBM10	V456M	Missense_Mutation	44.8
	ROS1	P1539L	Missense_Mutation	16.0
	SMO	V129I	Missense_Mutation	62.6
	TP53	R273C	Missense_Mutation	100.0
	TP53	-	CNA_DeepDel	-
	TRAF2	A168S	Missense_Mutation	52.1
	WT1	Q155H	Missense_Mutation	55.3
	ZFHX3	Q1740_Q1741del	In_Frame_Del	31.9
	ZFHX3	G3526_G3527dup	In_Frame_Ins	23.4
KP-MRT-YM	*ARID1A*	Y762*	Nonsense_Mutation	39.3
	AXIN1	D320N	Missense_Mutation	50.1
	CTNNB1	S33C	Missense_Mutation	42.5
	DOT1L	L974F	Missense_Mutation	47.6
	EIF4A2	I384T	Missense_Mutation	5.9
	EP300	H1261Y	Missense_Mutation	11.5
	HGF	R502L	Missense_Mutation	5.8
	SMARCB1	-	CNA_DeepDel	-
	TET1	S573_S575dup	In_Frame_Ins	22.2
KP-MRT-AN	*AXIN1*	V600M	Missense_Mutation	46.6
	CDH1	P126L	Missense_Mutation	49.3
	CDKN2AP14 ARF	-	CNA_DeepDel	-
	CDKN2AP16 INK4A	-	CNA_DeepDel	-
	CDKN2B	-	CNA_DeepDel	-
	EP300	G2218S	Missense_Mutation	99.9
	KMT2A	P3610L	Missense_Mutation	52.2
	MET	-	CNA_Amp	-
	MYCN	R357H	Missense_Mutation	5.1
	NOTCH1	R1296H	Missense_Mutation	49.8
	PIK3CG	P401L	Missense_Mutation	50.0
	RAD51	R150Q	Missense_Mutation	46.6
	RPTOR	P227L	Missense_Mutation	49.2
	SLX4	R481G	Missense_Mutation	50.4
	SMARCB1	-	CNA_DeepDel	-
	ZFHX3	G3527del	In_Frame_Del	72.2
MSKMRT-14531	*AXIN1*	R417H	Missense_Mutation	52.9
	EPHA5	E106G	Missense_Mutation	46.6
	FAT1	L3781P	Missense_Mutation	49.3
	HLA-A	X338_splice	Splice_Region	21.1
	KMT2D	G2141R	Missense_Mutation	45.9

	MAP3K1	E1286V	Missense_Mutation	47.6
	NCOA3	A1227T	Missense_Mutation	46.7
	NF2	T581P	Missense_Mutation	51.9
	SMARCB1	-	CNA_DeepDel	-
MSKMRT-31222	*MLH1*	Q60*	Nonsense_Mutation	14.0
	SMARCB1	-	CNA_DeepDel	-
	ZFHX3	G3526_G3527del	In_Frame_Del	22.4

Abbreviations: VAF, variant allele frequency; CNA, copy number alteration; Del, deletion; Amp, amplification; Ins, insertion.